Jurnal Mekanikal
December 2012, No.35 , 38-53

DOUBLE-EFFECT SOLAR ABSORPTION THERMAL ENERGY STORAGE

R.A. Rasih[1] and F.N. Ani[*2]

[1]Faculty of Mechanical Engineering,
Universiti Teknologi Mara Pulau Pinang,
13500 Permatang Pauh, Pulau Pinang

[2]Faculty of Mechanical Engineering,
Universiti Teknologi Malaysia,
81310 UTM, Johor Bahru

ABSTRACT

Solar radiation is a clean and renewable form of energy, which is required to be the main source of natural processes. Solar absorption refrigeration system (SARS) uses free source of energy when compared to the conventional electrical sources. This paper presents the SARS that is designed using meteorological data from Kuala Terengganu on 2004. The area which is located at 5°10'N latitude and 103°06'E longitude does experience a relative "dry season" from April through June, while the heaviest precipitation is seen at the end of the year, in November and December. The purpose of this project is to determine the performance of double-effect absorption chiller using solar energy through simulation approach. Initially, three types of solar collector were chosen but evacuated tube was selected as the main work due to its high efficiency. Solar energy is absorbed by the evacuated tube solar collector and then transferred to the hot water storage tank. High-pressure generator is driven by hot water storage system. The modeling and simulation of SARS is carried out using Matlab software package. Using equilibrium low-pressure generator temperature approach, the results show that minimum reference temperature of 130^oC is required to run the absorption chiller because the coefficient of performance (COP) will drop sharply below this temperature. Apart from that, the maximum COP of 1.2 is achieved at high-pressure generator temperature of 15^oC. 5 m^3 of hot water storage tank is required to achieve continuous operation of absorption chiller. The solar collector area was designed based on the solar fraction ranging from 50% to 90% monthly. The operational system for 100kW of refrigeration load in a year consists of 250 m^2 evacuated tube solar collector sloped at 2^o.

Keywords: *Solar absorption, lithium bromide-water, double-effect, equilibrium generator temperature, simulation.*

1.0 INTRODUCTION

Among the various thermal applications of solar energy, cooling system is one of the most complex concepts either in modeling or construction. Thus its utilization at present is not huge as water or space heating. A suitable device is required to convert solar energy into cold system. In order to produce cooling effect, it must be capable of absorbing heat at a low temperature from the conditioned space area and rejecting it into higher temperature of the outside air.

[*]Corresponding author : farid@fkm.utm.my

Apart from that, the best position of solar energy is available in two broad bands encircling the earth between 15° and 35° latitude north and south [1]. Malaysia is located to the next best position, which is the equatorial belt between 15°N and 15°S latitude. We believe that Malaysia has a potential to run the solar absorption cooling system based on the recommended solar irradiation value which is 4.39 kWh/m^2 for daily, 133 kWh/m^2 for monthly, and 1596.5 kWh/m^{-2} for standard yearly [2].

The study approach by numerical and simulation provides many advantages such as the expense of building prototypes can be eliminated, the system components can be optimized, the amount of energy delivered can be estimated, and the temperature variation of the system can be predicted. [3] investigated the performance of steady state double-effect absoprtion chiller through simulation study. According to their paper, the thermal performance of each chiller component is linearly increasing to the load factor. [4] conducted a simulation study for solar absorption cooling system in India. The study revealed that lower reference temperature (inlet generator temperature) gives better results for fraction of total load met by non-purchased energy (FNP). The reference temperature of 80^{o}C also recommended for single-effect absorption chiller system. [5] presented a comparative study on water and air-cooled solar absorption cooling systems. The study provided different kind of absorption cycle and working pair. The paper suggested that single lift half-effect was recommended to be the best low cost competitive solar cooling systems.

The performance characteristics of absorption chillers also discussed through simulation by [6], [7] and [8]. All of them focused on the single-effect of absorption chiller using TRNSYS simulation program. All of these studies stated that the maximum COP for single-effect varied from 0.7-0.8 with reference temperature of hot storage tank around 80^{o}C to 90^{o}C. The solar collector of flat plate with different tilt angle was used to provide solar energy for absorption system. The absorption chiller capacity used by these studies was ranged from 3.5kW to 16.5kW. However, none of them have interested to build a modular computer program for solar absorption system.

On the contrary, [9] build their own computer program for single-effect solar absorption system using meteorological data from Antalya, Turkey. They provided a detail solar energy process including the effect of hot water supplied from the solar energy, the effect of inlet temperature on the COP, and the effect of heat transfer surface area of the absorption coooling components based on a 10.5kW constant cooling load. The correlation equations were applied and three types of solar collector were considered which is flat plate (single glazed), flat plate (double glazed) and evacuated tube. Among these solar collectors, evacuated tube was selected as the best due to its high efficiency. However, the daily analysis is restricted from 10 am to 5 pm and monthly analysis is investigated from May to September only.

This study concentrates on the simulation of double-efffect solar absorption cooling system with a detail analysis of solar energy including thermal energy storage system. The paper presents the simulation of solar absorption system and thermal energy storage. The performance of the system also evaluated based on solar radiation data, solar collector type, hot water storage and absorption chiller system. In addition, the solar fraction relation with solar collector area is discussed in this paper. Three solar collectors were selected and analyzed from literature and the best is chosen based on its capability to give highest efficiency. Instead of using TRNSYS program to analyze system components, MATLAB codes are written to run the simulation.

2.0 SYSTEM DESCRIPTION

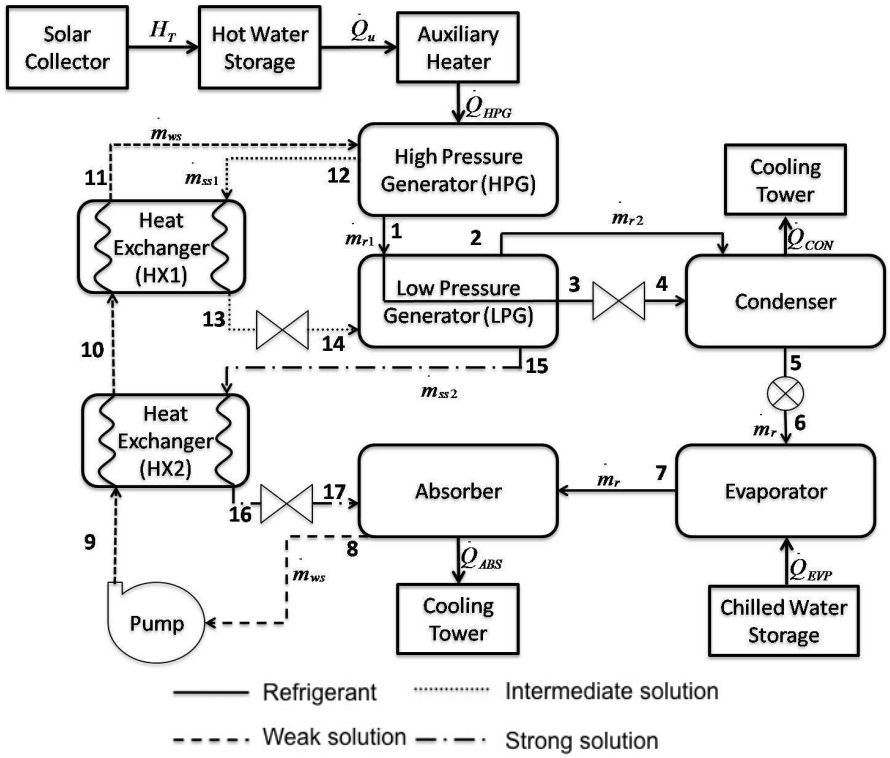

Figure 1: Schematic of double-effect solar absorption air conditioning system (series flow).

Figure 1 shows the schematic of double-effect absorption air chiller system. This system consists of four main flow circuits, which are solar collector, generator, cooling water and chilled water. The solar energy is absorbed by the solar collector and then hot water is produced. Hot water is accumulated in the storage tank before supplied to the high-pressure generator (HPG). As heat is absorbed from HPG, the weak solution (ws) increases its concentration into intermediate solution (ss1). All vapor generated at HPG (state 1) is fully condensed at the low-pressure generator (LPG). Orifice is installed to prevent the vapor in LPG from escaping to the condenser but allows condensate passes through it (state 3).

In the LPG, water vapor generated at HPG (state 1) supplies energy to boil off water vapor from Lithium-Bromide (LiBr) solution (state 14). Thus the LiBr solution concentration is increased (state 15) to become strong solution (ss2). The system is called as double-effect due to the energy supplied to the HPG is used twice (to boil off water vapor from weak solution and also intermediate solution). Water vapor from both generators (state 2, 4) is cooled down in the condenser (state 5) and then flowed to the evaporator (state 6). At the evaporator, the refrigerant (water) evaporated at low pressure (state 7), hence providing cooling effect to the chilled water. At the same time, the intermediate solution (ss1) leaving the HPG (state 12) passes through a primary heat exchanger (HX1) to preheat the weak solution (state 10) from the secondary heat exchanger. The intermediate solution (ss1) then passes through the LPG (state 15) to become strong solution (ss2) where the concentration of LiBr is higher than previous. The solution then passes to the secondary heat exchanger (HX2) to preheat the weak solution (state 9) from the absorber. In the absorber (state 17), the strong solution (ss2) absorbs the

water vapor (state 7) from the evaporator. The heat of condensation in the absorber is rejected to the cooling water from cooling tower. When the temperature in the storage tank is below than the required value (130°C), i.e. during evening or rainy days, the auxiliary heater is turned 'ON' to supply hot water at the storage tank. As a consequence, the absorption chiller cycle can be operated continuously throughout the days.

3.0 SOLAR ABSORPTION MODELING

Solar absorption system is categorized into two main systems which are solar circulation and absorption circulation.

3.1 Solar Circulation

Non-concentrated type (flat plate and evacuated tube) solar collectors are selected rather than concentrated solar collectors. This is due to the tracking control is required for concentrating collector (i.e. parabolic) and higher cost is produced. Some of the solar collectors parameters selected are shown in Table 1 as suggested by [10]:

Table 1: Types of selected solar collectors and its coefficients.

Type	Name	$(F_R)(U_L)$	$(F_R)(\tau\alpha)$
Class II	Evacuated tube element	2	0.73
Class III	Selective black flat plate (double glazed)	3.5	0.69
Class IV	Matt black flat plate (single glazed)	7.5	0.63

The best solar collector is chosen based on its capability to produce highest efficiency and solar heat gain. Under steady conditions, the useful heat delivered by a solar collector is equal to the energy absorbed in the heat transfer fluid minus the direct and indirect heat losses from the surface to the surroundings. This relation can be described by the solar collector efficiency, η_{col} and collector heat gain, Q_u as below [11].

$$\eta_{col} = (F_R)(\tau\alpha) - (F_R)(U_L)(T_{fi}-T_o)/G \quad (1)$$

$$Q_u = (\eta_{col})(A)(G) \quad (2)$$

In order to determine the solar collector area, solar fraction of the system need to be investigated. Solar fraction has been defined by [11] as:

$$f_i = L_{s,i}/ (L_{s,i} + L_{a,i}) \quad (3)$$

Where $L_{s,i}$ = Solar energy delivered [J]
$L_{a,i}$ = Auxiliary energy required [J]

Apart from that, solar collector must be tilted to some angle, β respected to the horizontal surface to maximize the absorption of solar radiation. Figure 2 shows the procedure to get the optimum tilt angle as suggested by [11]:

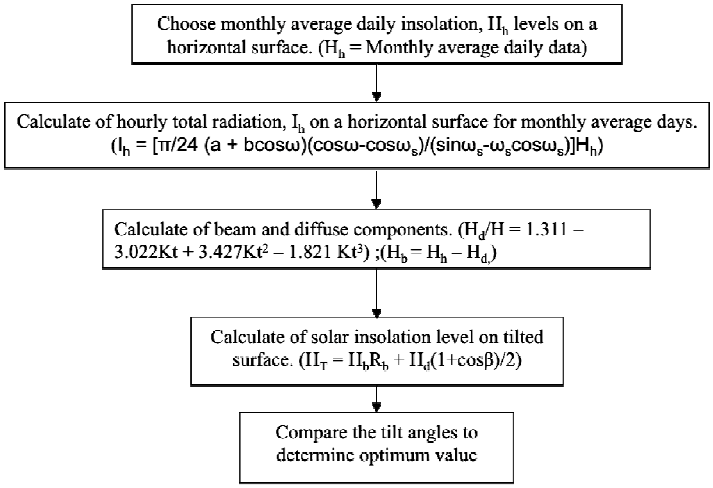

Figure 2: Tilt angle calculation procedure.

A water storage tank is placed after the solar collectors as shown in Figure 3. Well-mixed storage is assumed within the tank to simplify the analysis as shown in Figure 4. By assuming the rate of heat addition and removal in a reasonable time period, Δt is constant; the temperature inside the storage tank can be estimated as suggested by [11]:

$$T_{snew} = T_{sold} + (\Delta t / \dot{m}C_p)_s(\dot{Q}_u - \dot{Q}_l - \dot{Q}_{loss}) \quad (4)$$

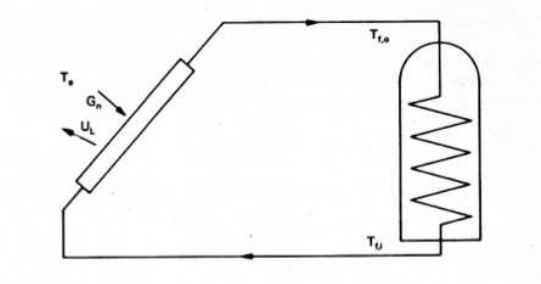

Figure 3: Thermal solar collector linked to storage tank.

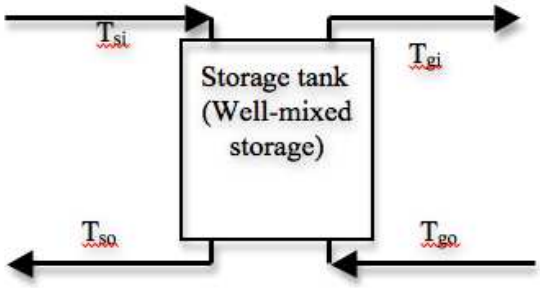

Figure 4: Well-mixed storage assumption in the storage tank

In the solar collector, the solar heat is transferred from the solar collector to the storage tank due to the temperature gradient. This heat also contributes to the heat addition into the storage tank:

$$\dot{Q}_u = (\dot{m}C_p)(T_{fo-}T_{fi}) = (\dot{m}C_p)(T_{si} - T_{so}) \tag{5}$$

The rate of heat loss inside the storage tank is calculated as:

$$\dot{Q}_{loss} = (UA)_s (T_{si} - T_{so}) \tag{6}$$

The rate of heat extraction to meet the generator load:

$$\dot{Q}_1 = (\dot{m}C_p)(T_{gi} - T_{go}) \tag{7}$$

3.2 Absorption Circulation

Based on Figure 1, the following assumptions are made for analysis at the absorption chiller:

i. Steady state and steady flow.
ii. Negligible kinetic and potential energy across each component.
iii. Only pure refrigerant boils in the water.
iv. Flow head losses in the piping system are negligible.
v. Constant pumping rate.
vi. The dilute solution leaving the absorber is in phase equilibrium at the same water vapor pressure as the refrigerant from the evaporator.
vii. Flow restrictors, such as expansion valves, spray nozzles, and the steam trap are adiabatic.
viii. The temperatures of superheated vapors leaving two generators have the same temperature as the concentrated solution leaving the high and temperature generator. The vapor leaving the generator has the equilibrium temperature of the weak solution at generator pressure.
ix. The vapor from high-pressure generator condenses fully at the low-pressure generator.
x. There are no convection and radiation heat losses through surfaces to ambient.

Equilibrium property correlations from literature are taken for water [12] while for lithium bromide-water solution is [13]. These correlations are required to obtain temperatures, pressures, enthalpies, and concentrations at various states of the system for water vapor and lithium bromide-water solution. The mass and energy balances for each component can be expressed as:

Condenser:

$$\dot{m}_{r1} + \dot{m}_{r2} = \dot{m}_r \tag{8}$$
$$\dot{Q}_{\text{CON}} = \dot{m}_{r1}h_3 + \dot{m}_{r2}h_2 - \dot{m}_r h_5$$

Evaporator:

$$\dot{m}_6 = \dot{m}_7 \tag{9}$$
$$\dot{Q}_{EVP} = \dot{m}_{r7} h_7 - \dot{m}_{r6} h_6$$

Absorber:

$$\dot{m}_{ws} = \dot{m}_r + \dot{m}_{ss2} \tag{10}$$
$$\dot{Q}_{ABS} = \dot{m}_r h_7 + \dot{m}_{ss2} h_{17} - \dot{m}_{ws} h_8$$

Generator

$$\text{LPG: } \dot{m}_{ss1} = \dot{m}_{ss2} + \dot{m}_{r2} \tag{11}$$
$$\dot{m}_{r1} h_1 + \dot{m}_{ss1} h_{14} = \dot{m}_{r2} h_2 + \dot{m}_{r1} h_3 + \dot{m}_{ss2} h_{15}$$

$$\text{HPG: } \dot{m}_{ws} = \dot{m}_{r1} + \dot{m}_{ss1} \tag{12}$$
$$\dot{Q}_{HPG} = \dot{m}_{r1} h_1 + \dot{m}_{ss1} h_{12} - \dot{m}_{ws} h_{11}$$

$$\text{COP = desired output/required input} \tag{13}$$
$$= \dot{Q}_{EVP} / \dot{Q}_{HPG} \qquad (\dot{W}_P << \dot{Q}_{HPG})$$

All the equations are solved simultaneously and the calculation procedure is shown in Figure 5:

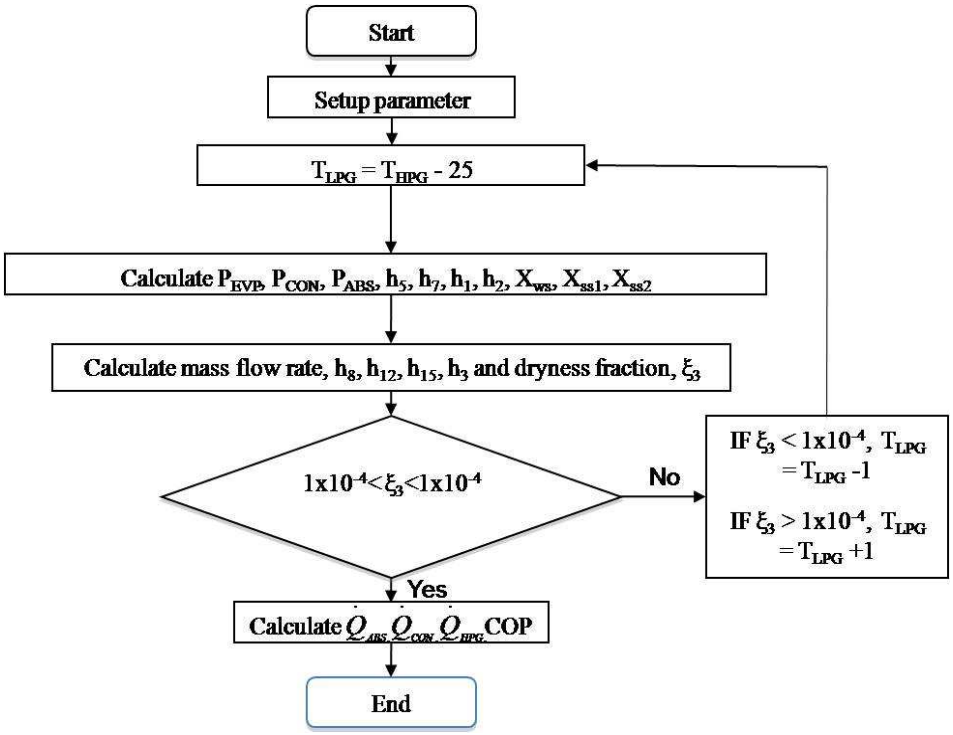

Figure 5: Flow chart for absorption chiller simulation.

4.0 RESULTS AND DISCUSSIONS

4.1 Weather Data

Meteorological data from Kuala Terengganu on 2004 [14] is used in this work. The variation of the average dry bulb temperature during 1 year is presented in Figure 6. As can be seen the maximum dry bulb temperature occurs in April and May and the temperature range between 27°C to 29°C. This data implies that the cooling demand is higher for April and May. However, the solar energy also increased during this period of time due to the higher hot water temperature can be supplied to the generator.

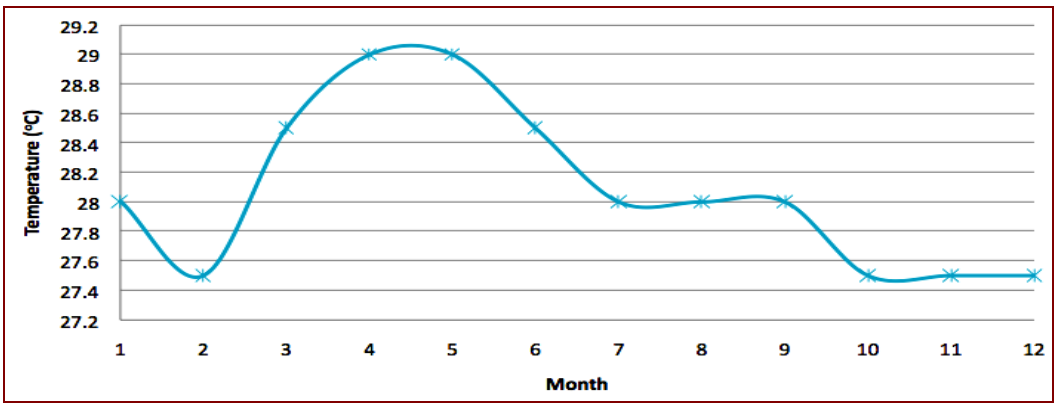

Figure 6: Monthly average variation of dry bulb temperature for Kuala Terengganu in 2004.

4.2 Solar Collector

Figure 7 shows the effect of different types of solar collector to the solar heat gain. Evacuated tube is selected due to its highest efficiency, which provides higher heat gain. However, to maximize the total solar radiation absorbed by the solar collector, it is required to deflect the angle of solar collector.

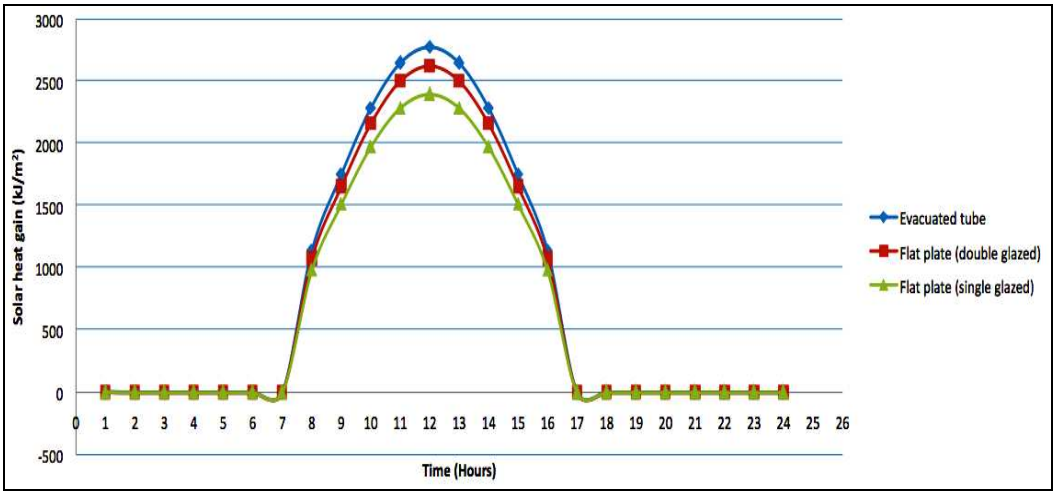

Figure 7: Solar heat gain for different types of solar collectors.

The tilt angle is varied from 0° to 50° from horizontal plane and Figure 8 shows the effect of this angle variation. From this comparison, the maximum radiation collected on the south facing surface is obtained with tilt angle value as high as 30° on January and

December and as low as 0° in most of the month (March to September). Generally, the maximum total radiation is received when the tilt angle (Beta = 30°) is applied during beginning and end of the year while horizontal surface of solar collector (Beta = 0^o) is applied in the middle of the year.

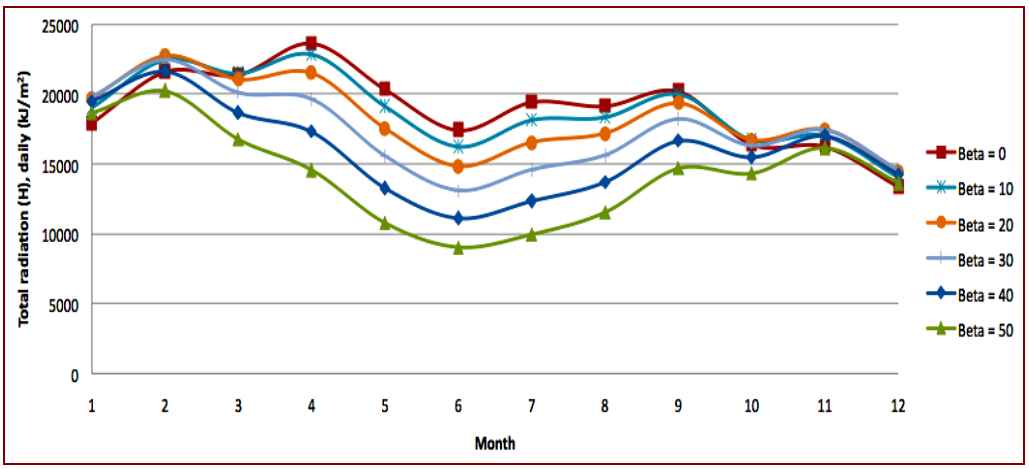

Figure 8: Total solar radiation on different tilted surface for each month.

On the other hand, changing the tilt angle to obtain optimum values throughout the year by daily and monthly does not seem to be practical. The alternative way to change the tilt angle once in a season [15] or once in a year. Matlab software package is used to plot the graphs by fitting the curve in second order polynomial. These polynomial equations are differentiated with respect to tilt angle and then equated to zero to obtain the optimum tilt angle corresponding to maximum insolation. Thus an optimum tilt angle is computed for the whole year at Kuala Terengganu station. Figure 9 shows the total radiation in Kuala Terengganu Station in year 2004 for different tilt angle.

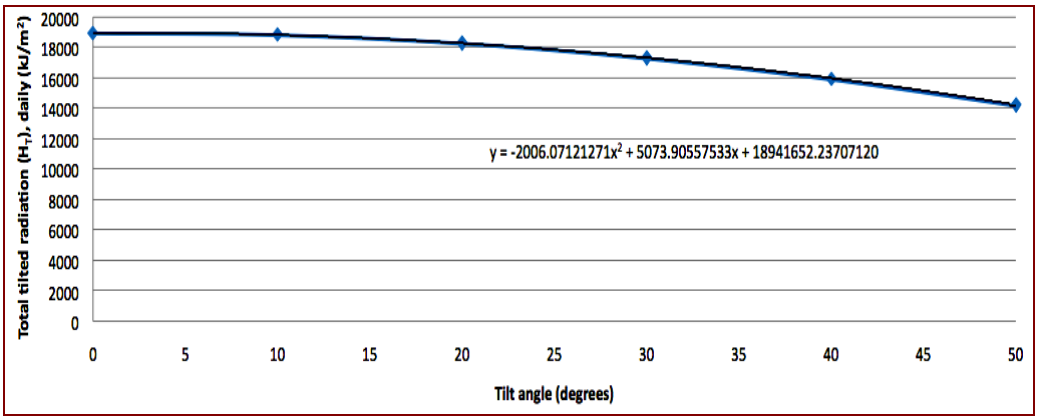

Figure 9: Total solar radiation in Kuala Terengganu Station (2004)

The optimum tilt angle is found to be 2° with the collector facing to the south direction. This result is in agreement with [16] who suggested that annual optimum tilt angle for small latitude region in the earth was closed to its location latitude (in this case 5° 10’ N).

Figure 10 shows the solar fraction for different value of solar collector area. It is clearly seen that as the solar collector area increases, the solar fraction also increases. However, the solar fraction is required to be lower than 1 so that no excessive heat is supplied to the absorption system. In addition, the solar fraction cannot be designed too

low because it will reduce the collection of solar energy and becomes uneconomical anymore. For this reason, the solar fraction is designed between 0.5 to 0.9. Thus solar collector area of 250 m^2 is chosen to run the absorption chiller.

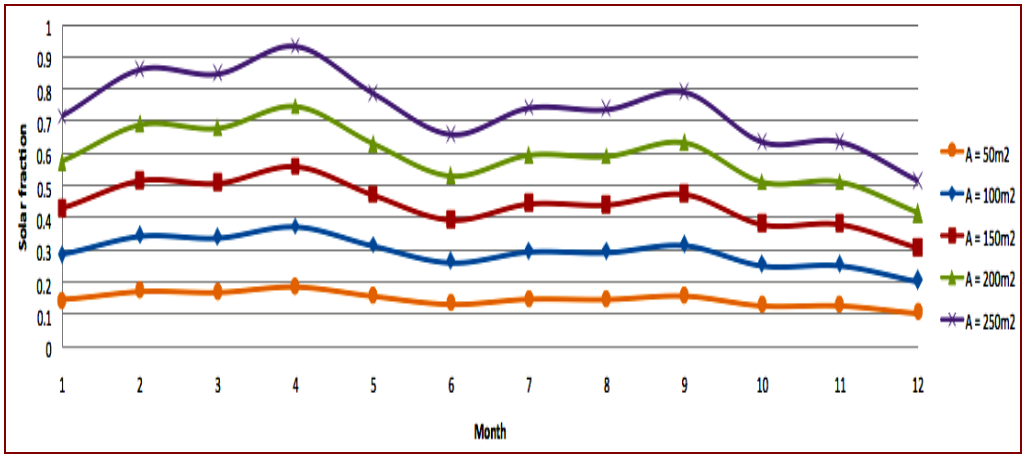

Figure 10: Solar fraction for different solar collector area.

This result basically can be evaluated using correlation equation [17]:

$$A_{spec} = 1 / (G_{max}.\eta_{col}.COP)$$
$$= 1/ (0.5422 \times 0.69 \times 1.2)$$
$$= 2.227 m^2/kW$$

Where G_{max} = Maximum solar irradiation in a year (kW/m^2)

η_{col} = Maximum solar efficiency in a year

Thus, for 100 kW the required value of solar collector area equal to 222.7 m^2 but the formula only gives very rough estimation based on the maximum value of solar irradiation and solar collector efficiency in a year.

4.3 Thermal Energy Storage

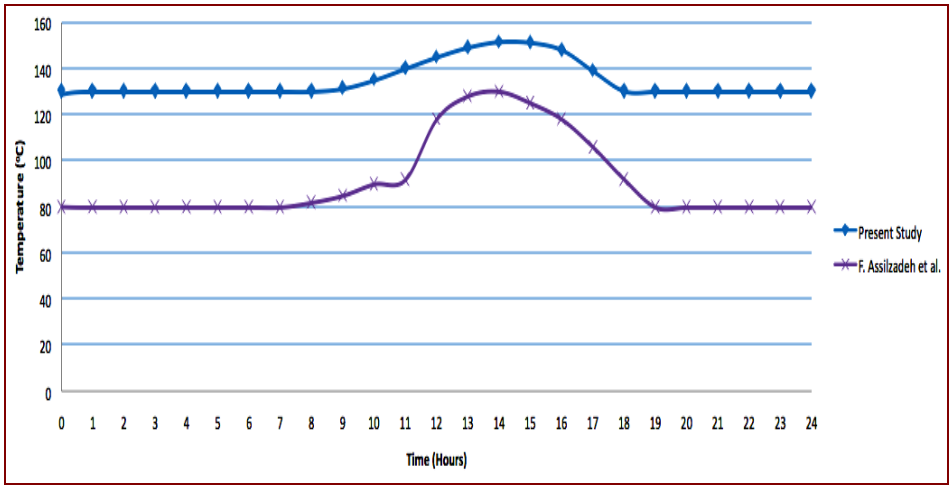

Figure 11: Hourly variation of storage tank temperature.

By assuming well-mixed storage, the behavior of a temperature for unstratified storage tank can be estimated using simple Euler integration. Figure 11 shows the variation of the storage tank temperature between present study and research done by [7].

The present study uses April 11th due to its highest solar energy gain from the solar radiation data collected. Load temperature from tank should not below 130°C because the COP of absorption refrigeration system will drop sharply below this reference temperature. To maintain this temperature, auxiliary heater is automatically switched ON by fix the minimum temperature in the tank as 130°C in the simulation. Based on this simulation result, the temperature is increased until 158°C; therefore, practically the pressurized tank is required to avoid steam generation. [7] have shown that only 80°C is required to be the reference temperature because the absorption type is single-effect while the present study runs a double-effect absorption system. Thus higher COP is achieved which indicate better performance.

4.4 Double-Effect Absorption Chiller System

In this system, the program code is run by using Matlab software package to determine the state of the working fluid in the absorption chiller system. By assuming high-pressure generator temperature to be 150°C, the simulation goes through 2877 iterations until the convergence of $1x10^{-2}$ is achieved. Temperature higher than 150°C will cause crystallization. Table 2 and Figure 12 show the states of working fluid in the absorption chillers after the simulation completed.

Table 2: States condition of the solar absorption chiller.

State	T (°C)	P (kPa)	h (kJ/kg)	X (% LiBr)	$\dot{m}$ (kg/s)
1	150	100	2782.8	0	0.0227
2	96.2	7.317	2681.6	0	0.0198
3	96.2	100	404.1	0	0.0227
4	96.2	7.317	404.1	0	0.0227
5	40	7.317	167.6	0	0.0425
6	40	1.2135	167.6	0	0.0425
7	10	1.2135	2519.4	0	0.0425
8	35	1.2135	76.1	52.6	0.2214
9	35	7.317	76.1	52.6	0.2214
10	59.9	7.317	129.1	52.6	0.2214
11	104.7	100	225	52.6	0.2214
12	150	100	325.5	58.6	0.1988
13	95.9	100	218.7	58.6	0.1988
14	80.9	7.317	218.7	58.6	0.1988
15	96.2	7.317	246.9	65.1	0.1789
16	59.5	1.2135	181.3	65.1	0.1789
17	59.5	1.2135	181.3	65.1	0.1789

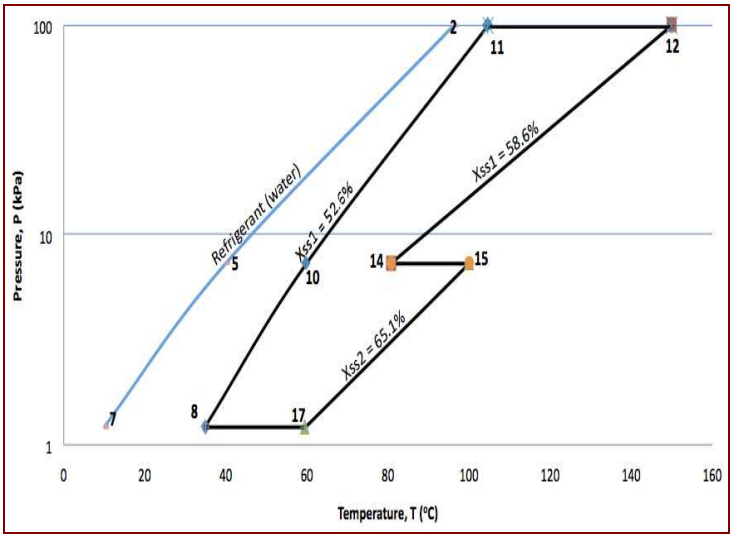

Figure 12: States of the solar absorption chiller.

Figure 13 shows the COP of the absorption chiller through different value of high-pressure generator temperature, T_{HPG}. It has been proven that for each absorption system, there was a minimum inlet generator temperature below, which it does not perform at all [18]. In this study, the minimum inlet generator temperature is found to be 130°C. The absorption chiller would not perform better below this reference temperature because the COP is too low. As can be seen from the graph, the COP increases sharply as the temperature increases, and then levels off to some asymptotic value.

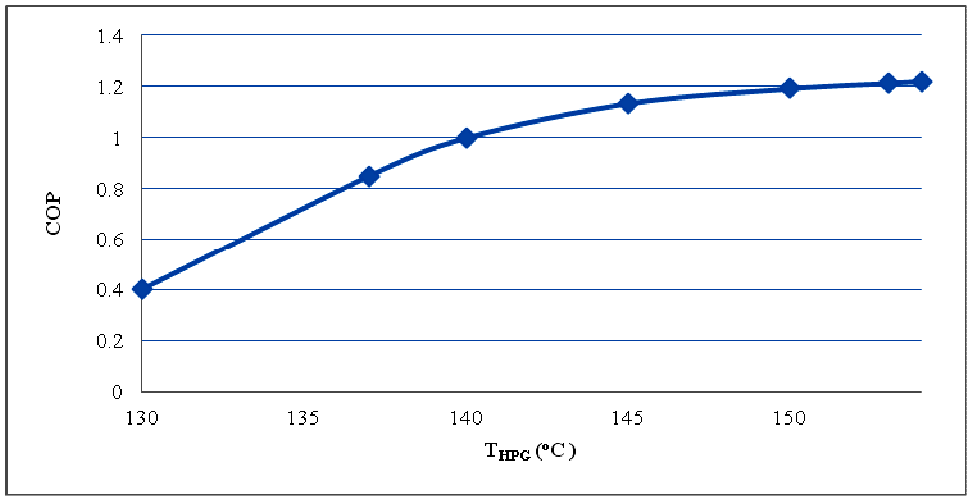

Figure 13: Coefficient of performance vs high-pressure generator temperature,T_{HPG}.

On the contrary, the COP can be improved by supplying higher generator temperature but it will cause another problem. As the higher generator temperature is supplied, the concentration of LiBr changes. This can be illustrated in Figure 14, which shows the concentration of LiBr for different value of generator inlet temperature.

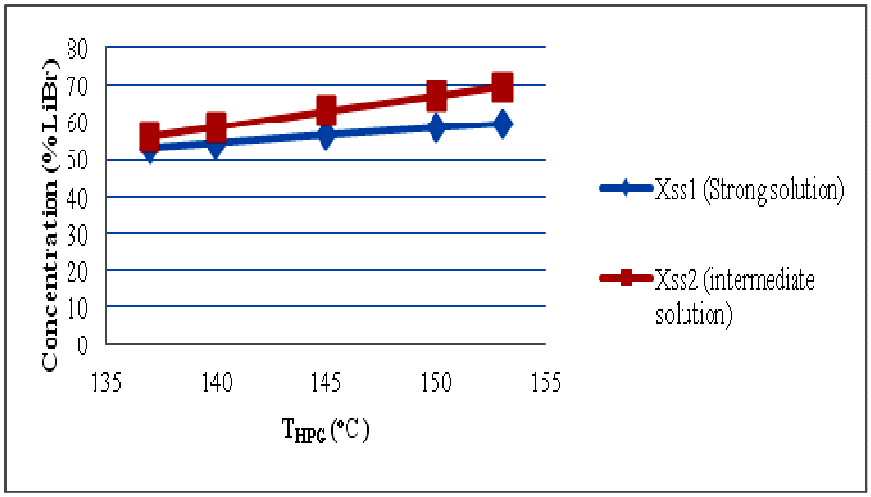

Figure 14: Concentration of LiBr, x vs high-pressure generator temperature, T_{HPG}.

It is clearly seen that the concentration of the LiBr increases when higher generator temperature is supplied to the system. As the crystallization limit for LiBr is around 70%, it is not desired to supply the generator temperature more than 150°C as the concentration of LiBr already reached 65%. Thus 150°C is the safe value that can be designed while maintaining 5% concentration gap before reach crystallization limit.

On the contrary, it is desired to have higher temperature at low-pressure generator so that more heat can be provided to run the absorption chiller. To understand this problem, Figure 15 illustrates the effect of low-pressure generator temperature for different value of high-pressure generator temperature.

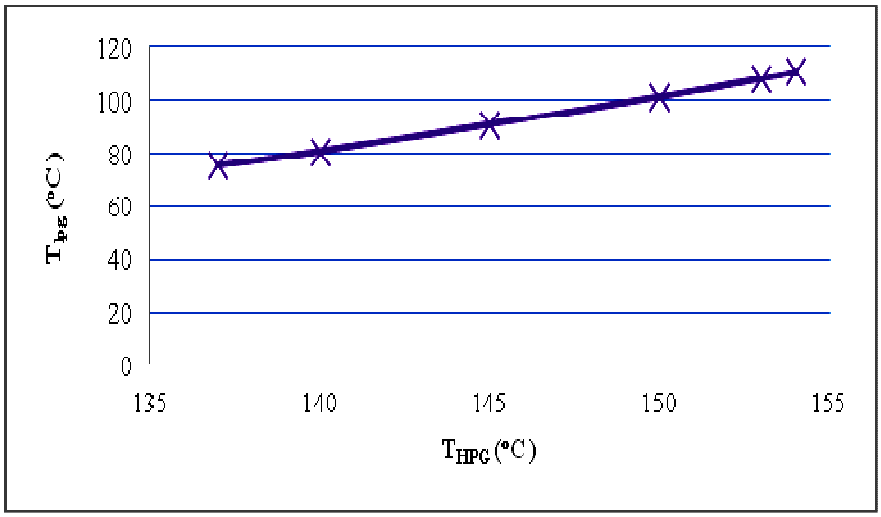

Figure 15 : Low-pressure generator temperature (T_{LPG}) vs high-pressure generator temperature (T_{HPG}).

It is obvious that the low-pressure generator temperature increases linearly with high-pressure generator temperature. More vapors are generated when T_{HPG} is increased. Since all the vapor from HPG has to be condensed in the LPG, more heat is available at LPG. As heat is transferred to the LPG, the T_{LPG} is increased to facilitate the condensation at HPG. As a consequence, a new equilibrium temperature and pressure at LPG is achieved. This temperature and pressure will counter the vapor generation in HPG and facilitating the condensation of vapor generation in LPG.

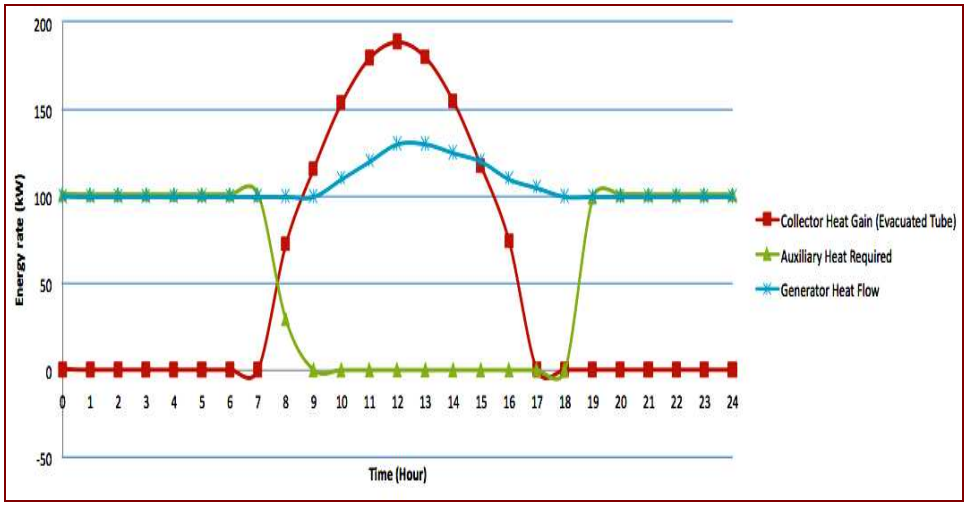

Figure 16: Energy rate flow of the solar absorption system.

After all of the absorption chiller components are analyzed, the energy flow that shows the heat gain of collector, auxiliary and generator of the solar absorption system is simulated. Figure 16 shows the system energy flows on April 11th from the solar radiation data obtained. A comparison of operation time for each component in the system can be clearly seen through this graph. As the solar collector is assumed to work only 10 hours from 7 am to 5 pm, the maximum of solar heat gain is found during 12 pm. Once heat is transferred to the storage tank at 7 am, the auxiliary heat starting to decrease until 9 am. At 9 am, the heat collected from 250 m^2 evacuated tube solar collector can sustain the refrigeration load of 100 kW. As a consequence, no auxiliary heat is required and the absorption chiller system is fully supported by the solar energy. When the solar collector absorbed excessive heat during noon, the generator load increases. Solar heat gain is no longer exist after 5 pm. However, 10 m^3 of hot water storage tank still contains some valuable heat and can support the refrigeration load from 5 pm to 6 pm. After that, auxiliary heater is automatically turned 'ON' to assist the hot water storage tank to supply the load demand from absorption chiller. After 9 pm, the refrigeration load is fully supported by auxiliary heater until the next day.

5.0 CONCLUSIONS

In the present study, the simulation for double-effect solar absorption thermal energy storage has been investigated. Solar thermal energy storage and absorption chiller system has been analyzed using Matlab software package and the following conclusions are obtained. Types of solar collector and solar radiation data affect the performance of solar collector. This study proved that evacuated tube provides better efficiency than flat plate solar collector. Secondly, solar collector area can be determined through solar fraction or correlation equation [17]. In this study, 250 m^2 evacuated tube is used to maintain the solar fraction between 0.5-0.9.

Besides, the COP of double-effect absorption chiller increases with high-pressure generator temperature before the value goes to an asymptote value of 1.2-1.3. If higher temperature source is available, triple-effect absorption chiller is suggested rather than double-effect. Higher temperature generator also can increase the COP but crystallization becomes the limitation.

Generally, the solar absorption system has a possibility to be used in Kuala Terengganu. However, the bad weather condition (i.e. wind monsoon) at the end of the

year becomes a big challenge to use the solar energy for absorption chiller. Economic evaluation analysis is recommended before run a full scale experimental here.

ACKNOWLEDGEMENTS

The authors wish to thank Universiti Teknologi Malaysia and the Malaysian Government for supporting this research activity.

NOMENCLATURE

A	Solar collector area, m^2
A_{spec}	Solar collector area specification, m^2/kW
C_p	Specific heat, kJ/Kg.K
f_i	Solar fraction, dimensionless
F_R	Heat dissipation factor, dimensionless
G	Solar irradiation, kJ/m^2
G_{max}	Maximum Solar irradiation, kJ/m^2
h	Specific enthalpy, kJ/kg
H_b	Beam solar radiation, kJ/m^2
H_d	Diffuse solar radiation, kJ/m^2
HPG	High pressure generator
HX1	Primary heat exchanger
HX2	Secondary heat exchanger
LPG	Low pressure generator
K_t	Clearness index, dimensionless
L_{si}	Solar energy delivered, kJ
L_{ai}	Auxiliary energy required, kJ
$\dot{m}$	Mass flow rate, kg/s
$\dot{Q}_u$	Rate of heat addition into the storage tank, kW
$\dot{Q}_{loss}$	Rate of heat loss into the storage tank, kW
$\dot{Q}_l$	Rate of heat extraction to meet the generator load, kW
$\dot{Q}_{HPG}$	Rate of heat generated at high-pressure generator, kW
$\dot{Q}_{LPG}$	Rate of heat generated at low-pressure generator, kW
$\dot{Q}_{CON}$	Rate of heat rejection at condenser, kW
$\dot{Q}_{EVP}$	Rate of heat absorbed at evaporator, kW
$\dot{Q}_{ABS}$	Rate of heat rejection at absorber, kW
ss1	Intermediate solution
ss2	Strong solution
T_s	Storage temperature, ^oC
T_{si}	Storage inlet temperature, ^oC
T_{so}	Storage outlet temperature, ^oC
T_{gi}	Generator inlet temperature, ^oC
T_{go}	Generator outlet temperature, ^oC
T_{fi}	Fluid inlet temperature, ^oC
T_{fo}	Fluid outlet temperature, ^oC
T_{snew}	New storage tank temperature, ^oC
Δt	Time period, s
U_L	Heat transfer coefficient, $W/m^2.K$
ws	Weak solution
X	Lithium Bromide concentration
α	Thermal diffusivity, m^2/s
β	Tilt angle, ^{o}

η_{col} Solar collector efficiency
τ Atmospheric transmittance, s/m^2

REFERENCES

1. Charles, E. B. (2002). *World Energy Resources.* USA: Springer.
2. Hussin, M. H. (2010). An Evaluation Data of Solar Irradiation and Dry Bulb Temperature at Subang Under Malaysian Climate . *IEEE Control and System Graduate Research Colloquium.* Photovoltaic Monitoring Centre (PVMC), Faculty of Electrical Engineering, Universiti Teknologi Mara, Malaysia.
3. Sid, M., Mohammed, A., Ahmed, S., & Ihtsh, S. (2010). Parametric Analysis of a Double-Effect Steam Absorption Chiller. *The 4th International Meeting of Advances in Thermofluids* . Melaka, Malaysia.
4. Mittal V, K. K. (2006). Modelling and Simulation of a Solar Absorption Cooling System for India. *Journal of Energy in Southern Africa, 17* (3).
5. Kim, D. I. (2009). Air-cooled LiBr–Water Absorption Chillers for Solar Air Conditioning in Extremely Hot Weathers. *Energy Conversion and Management, 50*, 1018-1025.
6. Balghouthi, M., Chahbanib, M., & A., G. (2008). Feasibility of Solar Absorption Air Conditioning in Tunisia. *Building and Environment, 43*, 1459-1470.
7. Assilzadeh, F., Kalogirou, S., Ali, Y., & Sopian, K. (2005). Simulation and Optimization of a LiBr Solar Absorption Cooling System with Evacuated Tube Collectors. *Renewable Energy* , 1143-1159.
8. Florides, G., Kalogirou, S., Tassou, S., & Wrobel, L. (2002). Modelling and Simulation of an Absorption Solar Cooling System for Cyprus.
9. Atmaca, I., & Yigit, A. (2003). Simulation of Solar Powered Absorption Cooling System. *Renewable Energy 28: 1277-1293, 2003, 28*, 1277-1293.
10. Simonson, J. (1984). *Computing methods in solar heating design.* Department of Mechanical Engineering, The City University London .
11. Duffie, J. A., & Beckman, W. A. (2006). *Solar Engineering of Thermal Process.* Solar Energy Laboratory, University of Wisconsion-Madison: John Wiley and Sons.
12. Liu, Y., & Wang, R. (2004). Performance Prediction of a Solar/Gas Driving Double Effect LiBr–H2O Absorption System . *Renewable Energy, 29*, 1677-1695.
13. ASHRAE. (2005). *Fundamental.*
14. Muzathik, A. M., Nik, W. M., Samo, K., & Ibrahim, Z. (2010). Reference Solar Radiation Year and SOme Climatology Aspects of East Coast of West Malaysia. *American J. of Engineering and Applied Sciences , 3* (2), 293-299.
15. Yakup, M., & Malik, A. (2001). Optimum Tilt Angle and Orientation for Solar Collector in Brunei Darussalam. *Renewable Energy, 24*, 223-234.
16. Siraki, A. G., & Pillay, P. (2012). Study of Optimum Tilt Angles for Solar Panels in Different Latitudes for Urban Applications. *Solar Energy* .
17. Lim, C., Sopian, K., & Sulaiman, Y. (2009). An Overview of Solar Assisted Air-Conditioning System Application in Small Office Buildings in Malaysia. *Proceedings of the 4th IASME / WSEAS International Conference on Energy and Environment*, (pp. 244-251). Solar Energy Research Institute, University Kebangsaan Malaysia, Malaysia.
18. Grossman, G. (2002). Solar Powered System for Cooling, Dehumidification, and Air-Conditioning. *Solar Energy Journal, 72*, 53-63.